RSC Advances

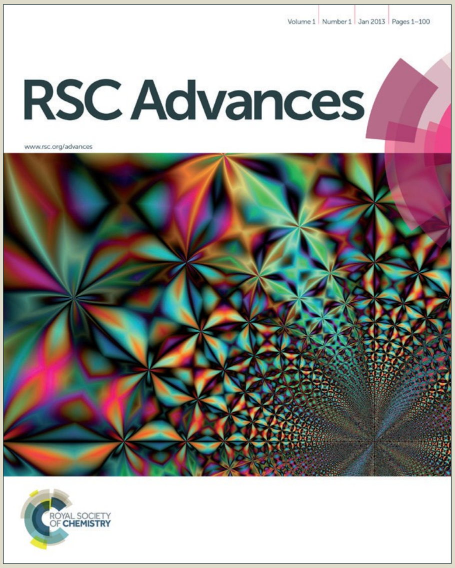

ROYAL SOCIETY OF CHEMISTRY

www.rsc.org/advances

Photocatalytic Degradation and Pathway of Oxytetracycline in Aqueous Solution by Fe_2O_3 - TiO_2 Nanopowders

Rong Li,[a] *Yuefa Jia ,*[a] *Jun Wu,*[a] *Qiang Zhen*[1a]

ABSTRACT

The degradation behavior of oxytetracycline (OTC) in aqueous solution using Fe_2O_3-TiO_2 nanopowders (Fe_2O_3-TiO_2 NPs) as photocatalyst under UV/visible light was investigated in this paper. Fe_2O_3-TiO_2 NPs photocatalysts synthesized using co-precipitation were characterized by XRD, TEM, FT-IR and UV-vis DRS. Fe_2O_3-TiO_2 NPs with 45 wt% Fe_2O_3 exhibited higher photocatalytic activity than others. The photocatalytic degradation of OTC shows maximum efficiency at pH=5.5 under both UV/visible due to the surface adsorption. The intermediate products during the photocatalytic degradation of OTC were detected by LC-MS/TOF. Six main intermediates were formed, and their evolution was discussed. On the basis of the evidence of oxidative intermediate formation and a detailed degradation path way of OTC by 45 Fe_2O_3-TiO_2 NPs are proposed.

Keywords: Fe_2O_3-TiO_2 NPs; photodegradation; OTC; LC-MS/TOF; degradation mechanism

---

[a] *Research Center of Nano Science and Technology, Shanghai University, Shanghai 200444, China.* [1] *E-mail address:* *qzhen@staff.shu.edu.cn(Qiang ZHEN), Tel: +86 21 66137276.*

1. Introduction

Antibiotic tetracyclines (TCs) are widely used in disease treatment for humans as well as disease prevention and as growth promoters in livestock. Among this family, oxytetracycline (OTC) is one of the most frequently detected tetracyclines in water bodies and sediments in many countries. Moreover, due to the antibiotic nature, hydrophilic property and stable naphthacene ring structure (seen in Figure 1), OTC is hardly removable by conventional water treatment process, including biological and chlorination process. Therefore, the spread of OTC in surface water may directly threaten the safety of drinking water for human consumption.

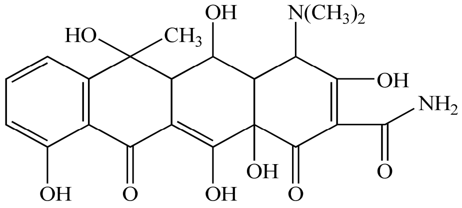

OTC: $C_{22}H_{24}N_2O_9$

Figure 1. Structure of OTC

Recently, photocatalytic degradation is considered as an affordable, effective, environment friendly technology to remove the antibiotic in aquatic system. Zhao *et al.*[1,2] has also studied the photocatalytic degradation of OTC using TiO_2-supported zeolite. As it is well know that TiO_2 alone can only response to ultraviolet light， thus limited its application. In order to improve the efficiency of solar energy utilization, visible light responsive (VLR) TiO_2 were developed. Among these materials, Fe_2O_3-TiO_2 composites exhibited excellent photocatalytic activity under visible light and were applied as photocatalyst in remove of various organic pollutants, such as auramine, acridine dye and aryl halides in solution.[3-5]

It is clear that the destruction of OTC is complicated; a series of intermediate products are formed during the photocatalytic process, and some may be more toxic than OTC. Thus, it is necessary to identify the intermediate products during the photocatalytic degradation, and further develop an understanding of the degradation mechanism. Liu *et al.*[6] suggested a possible degradation process of tetracycline (TC) using Cl-TiO_2 as photocatalysts and considered that the resulting ·OH radical can oxidize most of TC antibiotics to mineral end-products. However, the photocatalytic degradation pathway and mechanism of OTC has been few reported.

The present study attempts to assess the heterogeneous photocatalytic degradation of OTC by Fe_2O_3-TiO_2 NPs under UV and visible light, and further investigated the degradation behavior of OTC. Fe_2O_3-TiO_2 NPs were synthesized by co-precipitation, and characterized by XRD, TEM, FT-IR and UV-vis DRS. The effects of Fe_2O_3 content, initial pH of solution on degradation efficiency were investigated under UV/visible light, and compared to pure TiO_2. The main intermediate products formed during photocatalytic degradation process were analyzed by LC-MS/TOF. And based on these results, the detailed degradation pathway of OTC using 45 Fe_2O_3-TiO_2 NPs is proposed.

2. Experimental Section

2.1. Preparation of Fe_2O_3-TiO_2 NPs

Fe_2O_3-TiO_2 nanopowders were synthesized using co-precipitation method.[7] Certain amounts of predetermined $Fe(NO_3)_3·9H_2O$ and Ti $(SO_4)_2$ were dissolved in 10 ml dilute sulfuric acid, respectively, then both were poured into 400 ml ethanol to form a mixed solution. Aqueous ammonia(NH_3：25~28wt%) was added drop by drop in this mixed solution with continuous stirring. The pH of solution was controlled at 9 during the dropping process. The precipitate was firstly aged for 2 h, then filtered and washed till that no SO_4^{2-} was detected with Ba^{2+}. The precipitate was dried at 100 °C for 24 h, and calcined at 550 °C for 6 h to obtain Fe_2O_3-TiO_2 NPs.

2.2. Photocatalytic degredation of OTC

Photocatalytic degradation of oxytetracycline (OTC, 95% purity, Aladdin Chemistry Co., Ltd, Shanghai, China) was carried out quartz glass tubes (Φ=30 mm, H=260 mm), which was opened to the ambient air in order to reach the air-equilibrated condition. The reaction of unit used in this work was arranged as reported in literature. [3] A 300 W high-pressure mercury lamp was used as a UV light source, with main wavelength of 250 nm–400 nm. A 300 W iodine tungsten lamp was used as visible light source. The top of the quartz glass tube was 10 cm away from the UV and visible source.

Fe_2O_3-TiO_2 NPs photocatalysts at the dose of 1g/L was dispersed into OTC aqueous solution (60 mg/L) and shaked vigorous by using magnetic stirrer. The pH value of the solution was adjusted with hydrochloric acid or sodium hydroxide buffer solution to the desired value (pH = 2.0, 5.5, 8.5 and 11.0). A pH meter (PHS-25, Shanghai, China) was used to measure the pH value. Before switching on irradiation, OTC solution was continuously stirred (stirring speed: 500 r/min) in the dark for 1h to ensure adsorption-desorption equilibrium. Then the system was exposed under UV or visible light for different time. Each photocatalytic degradation experiment was conducted in triplicate. The reusability experimental of Fe_2O_3-TiO_2 NPs was similar to A. K. Patra *et al.*[8] reported.

After irradiation, 5 ml of the suspension was extracted and centrifuged, and the residual concentration of OTC was measured using a UV-Vis spectroscopy (Techcomp ltd. U3010, Japan) at its maximum absorption of 350 nm.[25] The photocatalytic degradation efficiency (DE) was calculated by the following formula (equation 1):

$$\mathrm{DE} = (\mathrm{A}_0 - \mathrm{A}_t) / \mathrm{A}_0 \times 100\% \qquad (1)$$

Where A_0 is the initial absorbance of OTC solution, A_t is the absorbance of OTC solution at the irradiation time (t).

2.3. Characterization

The phases of obtained Fe_2O_3-TiO_2 NPs and commercial Fe_2O_3, TiO_2 reagents were analyzed by X-ray diffraction (Rigaku D/Max-2200, Japan). The average crystalline size of Fe_2O_3-TiO_2 NPs nanopowder was calculated by Scherrer Equation (equation 2):

$$D = \frac{K\lambda}{\beta\cos\theta} \qquad (2)$$

Where D is the average crystalline size, K refers to a constant of 0.89, β is the integration of half-height width, θ is diffraction angle, and λ is X-ray wavelengths (equals to 0.15418 nm).

The micrography of 45 Fe_2O_3-TiO_2 NPs was observed via a transmission electron microscopy (Jeol 200CX, Japan). Infra-red (IR) spectra of 45 Fe_2O_3-TiO_2 NPs was recorded with a Nicolet Avatar 370 FT-IR (Thermo Nicolet, Waltham, USA). The UV-vis absorption spectra of photocatalysts were recorded by a UV-vis spectrophotometer (Techcomp ltd. U3010, Japan). Zeta potential of Fe_2O_3-TiO_2 NPs was measured with a nanoparticles and potential analyzer (Zetasizer 3000HS, United Kingdom).

LC-MS/TOF systems consisted of an Agilent 1260 infinity HPLC coupled with PDA detector and an Agilent 6230 Accurate Mass MS/TOF mass spectrometer (Agilent technologies singapore(sale)pte, America) were used for the structure information of unknown intermediary products formed during the photocatalytic degradation process. Each mass spectrometer was equipped with electrospray ionization (ESI) interface and operated in positive ionization mode. The mobile phase was acetonitrile and a representative separation of OTC was achieved within 13 min.

The MS full scan spectra with accurate mass determination were obtained by Agilent 6230 TOF mass spectrometer. Ionization condition conditions: drying gas (N_2) flow rate, 10.0 L/min; dry temperature, 330 °C; nebulizer, 30 psi; fragmentor, 130 V; capillary voltage, 4000 V; skimmer potential, 50 V; hexapole RF, 250 V. The TOF spectra were set to scan a mass range of 100-3200 m/z. All the operations, acquisition and analysis were controlled by Mass Hunter Workstation.

3. Results and Discussion

3.1 Characterization of Fe_2O_3-TiO_2 NPs

Figure 2(a) presents XRD pattern of anatase TiO_2 (anatase TiO_2 content is 99.8%, particle size of 60nm. Aladdin Chemistry Co., Ltd, Shanghai, China), hematite Fe_2O_3 (hematite Fe_2O_3 content is 99.5%, particle size of 30nm. Aladdin Chemistry Co., Ltd, Shanghai, China) and 45 Fe_2O_3-TiO_2 NPs. The main phases in 45 Fe_2O_3-TiO_2 NPs are anatase TiO_2 and hematite Fe_2O_3. The crystalline size of Fe_2O_3 and TiO_2 are 18nm and 14 nm calculated from Scherrer Equation, respectively. In addition, the micrography of 45 Fe_2O_3-TiO_2 NPs obtained is shown as Figure 2(b). The average particle size is around 20 nm, and well dispersed.

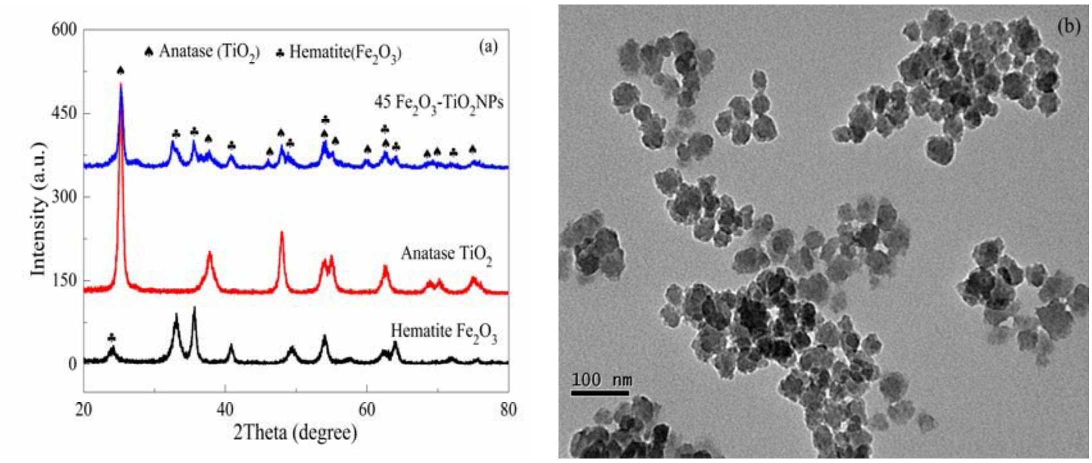

Figure 2. (a) XRD patterns of anatase TiO_2, hematite Fe_2O_3 and 45 Fe_2O_3-TiO_2 NPs, (b) TEM photo of 45 Fe_2O_3-TiO_2 NPs .

FT-IR spectra of 45 Fe_2O_3-TiO_2 NPs is shown in Figure 3(a). Bands at 3420.78 cm^{-1} and 1650.15 cm^{-1} are ascribed to hydroxyl.[9] While the strong absorption at 471.05 cm^{-1} is attributed to the stretching vibrations of the Ti-O in anatase TiO_2.[10]

Figure 3(b) shows the UV/vis absorption spectra of 45 Fe_2O_3-TiO_2 NPs, pure anatase TiO_2 and hematite Fe_2O_3. Anatase TiO_2 only absorbed ultraviolet radiation of less than 400 nm, while hematite Fe_2O_3 exhibits a high energy absorbance in the visible light region of 400-600 nm. The 45 Fe_2O_3-TiO_2 NPs shows not only stronger absorption in the ultraviolet region of less than 400 nm but also adequate and strong absorption in the visible light region of 400-600 nm. It indicates that 45 Fe_2O_3-TiO_2 NPs can also be used under visible light.

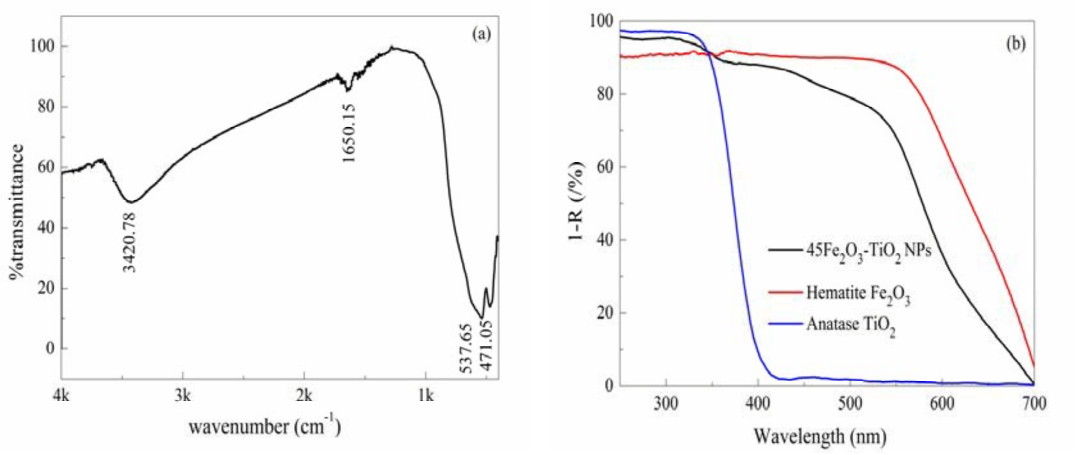

Figure 3. (a) FTIR spectra of 45 Fe_2O_3-TiO_2 NPs, (b) the UV/vis absorption spectra of 45 Fe_2O_3-TiO_2 NPs, anatase TiO_2 and hematite Fe_2O_3.

3.2 Effect of Fe_2O_3 content on photocatalytic activity

The representative UV-visible (vis) spectra changes of the OTC solution as a function of reaction time under UV condition were shown in Figure 4(a). The result shows that the adsorption peaks significant reduced with the increase of the irradiation time at 350 nm in 5 h.

Figure 4(b) illustrated the dependence of different Fe_2O_3 content on photocatalytic degradation efficience (DE) of OTC under UV light. All Fe_2O_3-TiO_2 NPs exhibited lower photocatalytic actvity than pure TiO_2, but much higher than pure Fe_2O_3. The photocatalytic activity of Fe_2O_3-TiO_2 NPs was found firstly increased with the increase of Fe_2O_3 content from 40 to 45 wt%. The 45 Fe_2O_3-TiO_2 NPs exhibited the highest photocatalytic DE of OTC. With the further increase of Fe_2O_3 content to 55%, the DE of OTC decreased slightly. Liu *et al.* [3] considered the recombination of electron-hole pairs was reduced due to combining Fe_2O_3 with TiO_2, and resulted in an increase of photocatalytic activity. However, when the content of Fe_2O_3 is higher than 45%, the surface of TiO_2 could have been covered with part of Fe_2O_3 of high concentration, and led to a decrease of light absorption activated site at the surface of TiO_2.

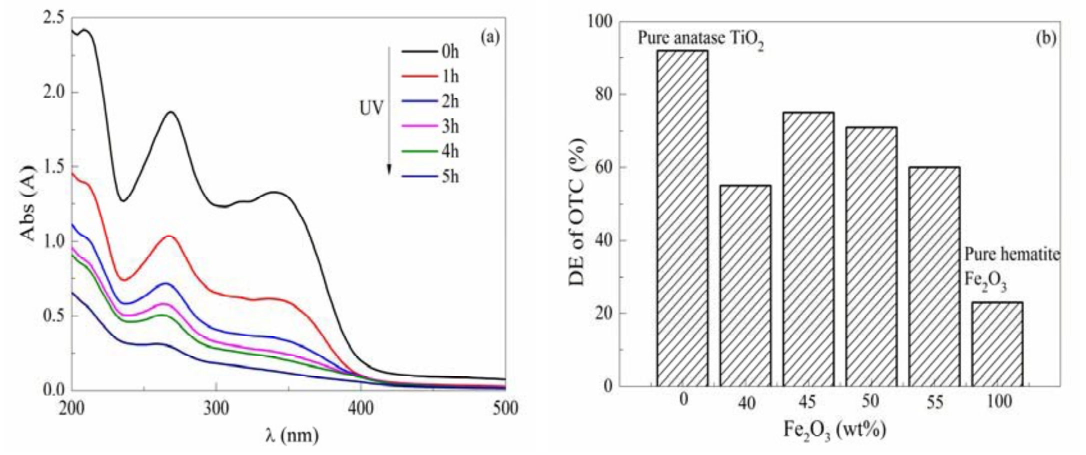

Figure 4. (a) UV-vis spectal changes of OTC solution with reaction time; (b) DE of OTC using Fe_2O_3-TiO_2 NPs, TiO_2 and Fe_2O_3 under UV light (OTC: 60 mg/L, pH = 2. Holding time: 5 h, the photocatalyst concentration was 1 g/L).

3.3 Effect of pH on OTC degradation

It has been reported that OTC has four species at different pH ranges[11], and each species has unique electric charge state. At pH = 2.0, OTC is protonated as H_3OTC^+. When pH is increased to 5.5, the majority of OTC changed to $H_2OTC^{\pm}$. Besides, OTC at pH 8.5 is primarily represented for the fraction of $HOTC^-$ while OTC mainly exists as OTC^{2-} at pH=11.0. Thus the initial pH of solution may affects photocatalytic degradation of OTC under both UV and visible. The effect of pH on photocatalytic degradation of OTC using 45 Fe_2O_3-TiO_2 NPs under both UV and visible light are presented as a function of irradiation time in Figure 5(a) and (b), respectively. The results showed that DE of OTC was firstly improved with increasing pH, then significantly lowered at pH=8.5and 11.0 under both UV and visible light.

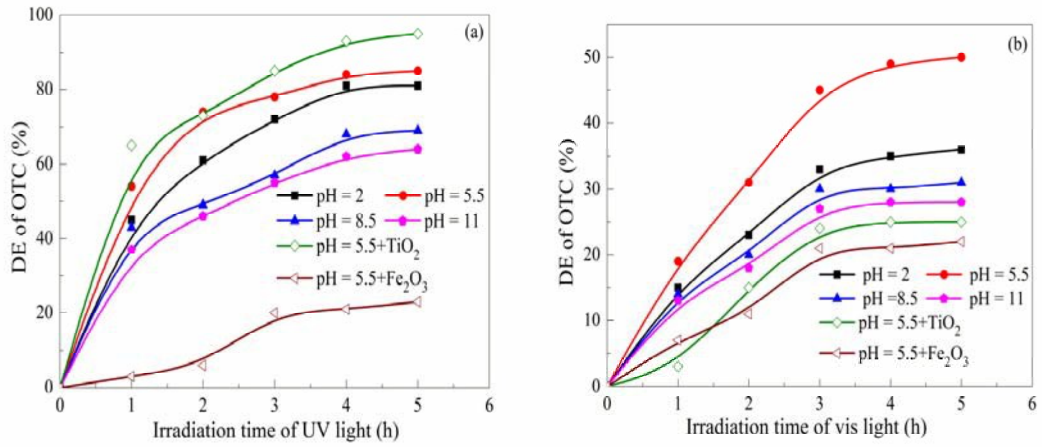

Figure 5. Effect of pH on DE of OTC (60 mg/L) under (a) UV and (b) visible light by

45Fe_2O_3-TiO_2 NPs ([45Fe_2O_3-TiO_2 NPs] = 1 g/L)

Figure 6(a) illustrates the effects of pH on the adsorption for OTC by 45 Fe_2O_3-TiO_2 NPs. The experiment was conducted in darkness, the initial concentration of OTC was 60 mg/L and the reaction time was 5h. As seen in Figure 6(b), the percent adsorption of OTC by 45 Fe_2O_3-TiO_2 NPs increased from 25% to 33% with increase in pH from 2 to 5.5, and decrease from 33% to 4% with increasing pH. This tendency was in good agreement with photocatalytic degradation behavior, indicating that the photocatalytic process was limited by the adsorption of OTC at the surface of catalyst in this experiment.

Figure 6(b) gives the pH-dependent zeta potential of 45 Fe_2O_3-TiO_2 NPs, and the zero point is around 8. When pH is higher than zero, 45 Fe_2O_3-TiO_2 NPs is negatively charged. As mention above, OTC mainly exists as $HOTC^-$ at pH = 8.5, OTC^{2-} at pH = 11, the electric repulsion makes the adsorption difficult, and leads to the decrease in OTC degradation. When pH is less than zero point, the surface of 45 Fe_2O_3-TiO_2 NPs, presents positive charge. At pH = 5.5, OTC acts as neutral- zwitterionic ($H_2OTC^{\pm}$) may result in relatively stronger adsorption of OTC on the surface of 45 Fe_2O_3-TiO_2 NPs, and sharply increase the OTC degradation. At pH = 2, the H_3OTC^+ is difficult to be absorbed on the positive surface. However, more OH^- absorbed on the surface of photocatalysts, generated more ·OH and enhanced the photo-catalytic degradation.

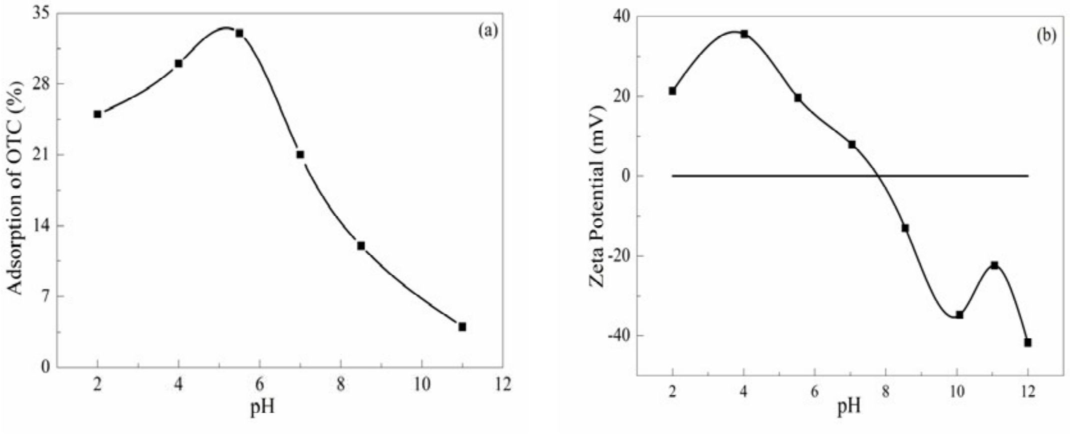

Figure 6. Effect of pH on (a) adsorption of OTC (60 mg/L, 5 h) by 45 Fe_2O_3-TiO_2 NPs, (b) zeta potential of 45 Fe_2O_3-TiO_2 NPs([45Fe_2O_3-TiO_2 NPs] = 1 g/L) under dark.

The photocatalytic degradation efficiency of OTC using pure TiO_2 and Fe_2O_3 at pH=5.5 are also given in Figure 5. Under UV light irradiation, photocatalytic activity of pure TiO_2 was superior to the 45 Fe_2O_3-TiO_2 NPs, but under visible light, the photocatalytic activity of 45 Fe_2O_3-TiO_2 NPs was significantly higher than pure TiO_2. Since visible light takes 50% of solar light, 45 Fe_2O_3-TiO_2 NPs are good candidates for further application in photocatalytic degradation OTC.

3.4 Reusability of 45 Fe_2O_3-TiO_2 NPs

In order to evaluate the potential applications, the reusability 45 Fe_2O_3-TiO_2 NPs has been studied under same conditions for 3 cycles, and the results are shown in Figure 7. Under both UV and visible light, the photocatalytic degradation of OTC decreased slightly during 3 cycles, showing that it could be used as an effective material for many cycles.

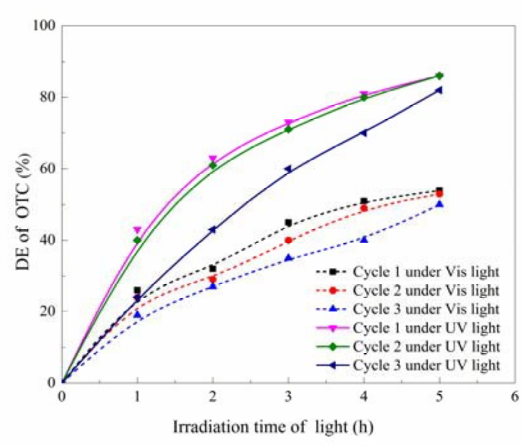

Figure 7. Photocatalytic activities 45 Fe_2O_3-TiO_2 NPs ([45Fe_2O_3-TiO_2 NPs] = 1 g/L) for the degradation of OTC (60 mg/L) at pH = 5.5 under UV/vis light for 3 cycles.

3.5 Analysis of degradation intermediates

The total ion chromatogram (TIC) of mass spectra for the samples of OTC solution before and after photocatalytic degradation is given in Figure 8. On the basis of this experiment result, the intermediate products during the photocatalysis process are identified by MS/TOF, and iron spectra at different retention time (RT) of OTC photocatalysis sample before and after 5h are presented in Supporting Information Figure S1.

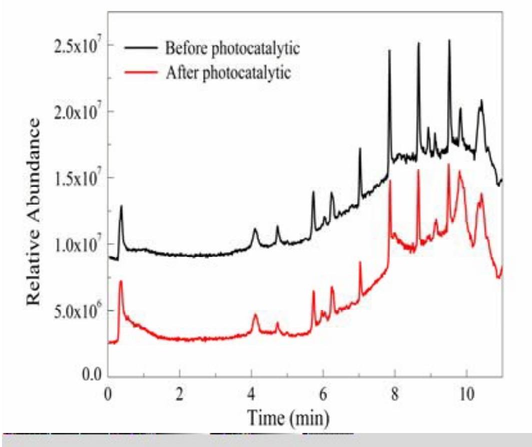

Figure 8. The total ion chromatogram (TIC) of mass spectra for OTC before and after photocatalytic degradation ([45 Fe_2O_3-TiO_2 NPs] = 1 g/L, OTC: 60 mg/L, pH = 5.5, 5 h UV/vis irradiation)

Five irons spectra at RT = 0.345, 0.354, 0.38, 4.882 and 6.656 min were detected in original OTC solution. The average mass spectra corresponding to these five irons are shown in Figure 9, five main product ions at m/z 477.1501 ($[M+H]^+$), m/z 461.1549 ($[M+H]^+$), m/z 447.1386 ($[M+H]^+$), m/z 446.1445 ($[M+H]^+$), and m/z 465.1294 ($[M+Na]^+$) might be identified as $C_{22}H_{24}N_2O_{10}$ (P_6), $C_{22}H_{24}N_2O_9$ (OTC), $C_{21}H_{22}N_2O_9$ (P_1), $C_{22}H_{23}NO_9$ (P_2) and $C_{22}H_{22}N_2O_8$ (P_3).

In the OTC solution after photocatalytic degradation under UV/vis irradiation, P_1, P_6 and OTC are not detected, while P_2 at m/z 446.1443 and P_3 at m/z 465.1294 are still remained. Besides, three evident product ions at m/z 415.149 ($[M+H]^+$), m/z 402.1188 ($[M+H]^+$) and m/z 179.0349 ($[M+H]^+$) are observed in the average mass spectra at 0.354 min, 5.706 min and 10.423 min, which are different from other main product ions in this experiment. Based on the molecular weight of the compound we therefore suggested that these peaks represent $C_{21}H_{22}N_2O_7$ (P_4), $C_{20}H_{19}NO_8$ (P_5) and $C_9H_6O_4$ (P_7). It was suggested that these three products were formed during the photocatalytic degradation process.

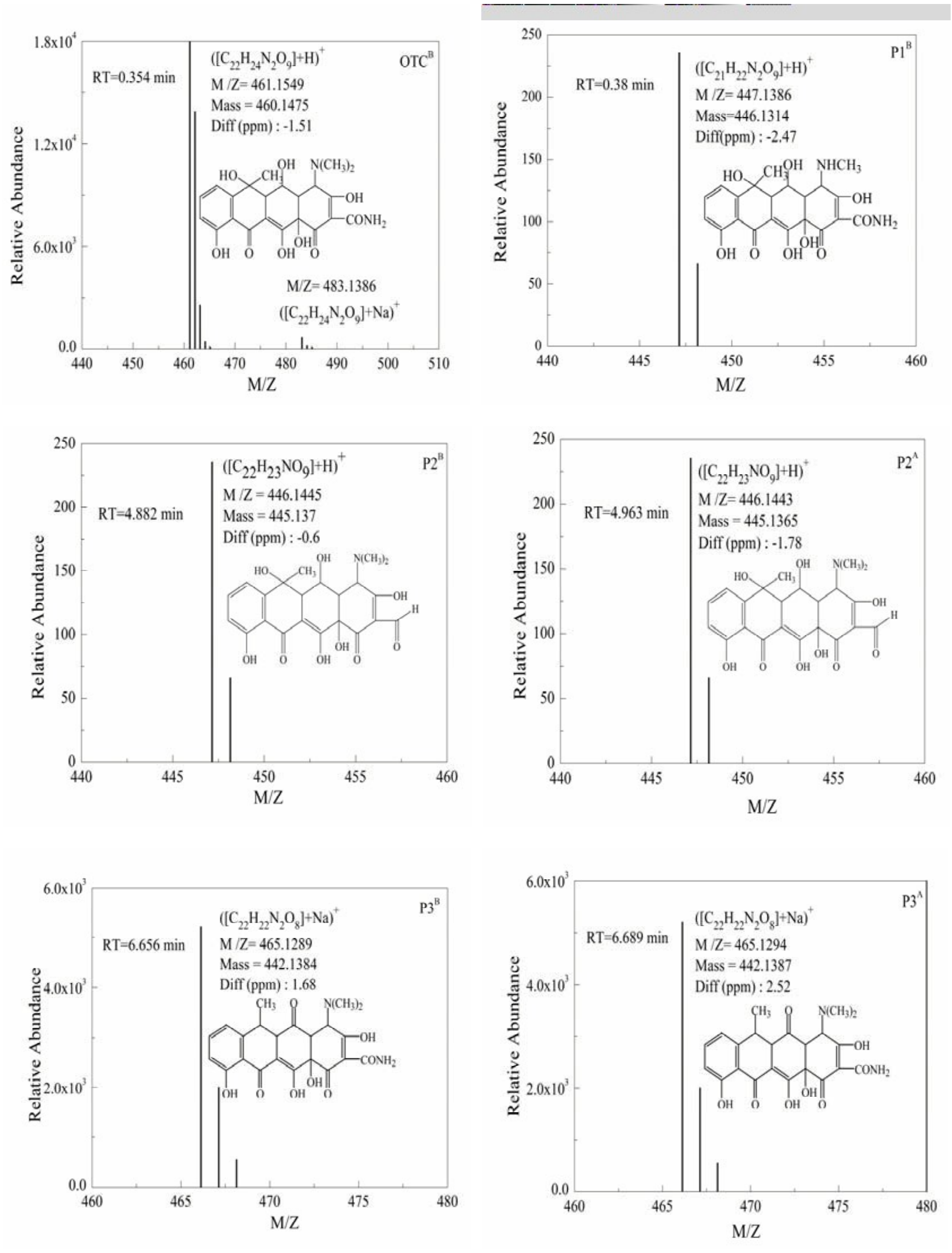
1.8x10^4
1.2x10^4
6.0x10^3
0.0
Relative Abundance
RT=0.354 min
([C22H24N2O9]+H)+
M /Z= 461.1549
Mass = 460.1475
Diff (ppm) : -1.51
OTC^B
HO CH3 OH N(CH3)2 OH CONH2 OH O OH OH O
M/Z= 483.1386
([C22H24N2O9]+Na)+
440 450 460 470 480 490 500 510
M/Z
250 200 150 100 50 0
RT=0.38 min
([C21H22N2O9]+H)+
M /Z= 447.1386
Mass=446.1314
Diff(ppm) : -2.47
P1^B
HO CH3 OH NHCH3 OH CONH2 OH O OH OH O
440 445 450 455 460
M/Z
RT=4.882 min
([C22H23NO9]+H)+
M /Z = 446.1445
Mass = 445.137
Diff (ppm) : -0.6
P2^B
HO CH3 OH N(CH3)2 OH H OH O OH OH O O
RT=4.963 min
([C22H23NO9]+H)+
M /Z= 446.1443
Mass = 445.1365
Diff (ppm) : -1.78
P2^A
6.0x10^3
4.0x10^3
2.0x10^3
0.0
RT=6.656 min
([C22H22N2O8]+Na)+
M /Z= 465.1289
Mass = 442.1384
Diff (ppm) : 1.68
P3^B
CH3 O N(CH3)2 OH CONH2 OH O OH OH O
460 465 470 475 480
M/Z
RT=6.689 min
([C22H22N2O8]+Na)+
M /Z= 465.1294
Mass = 442.1387
Diff (ppm) : 2.52
P3^A

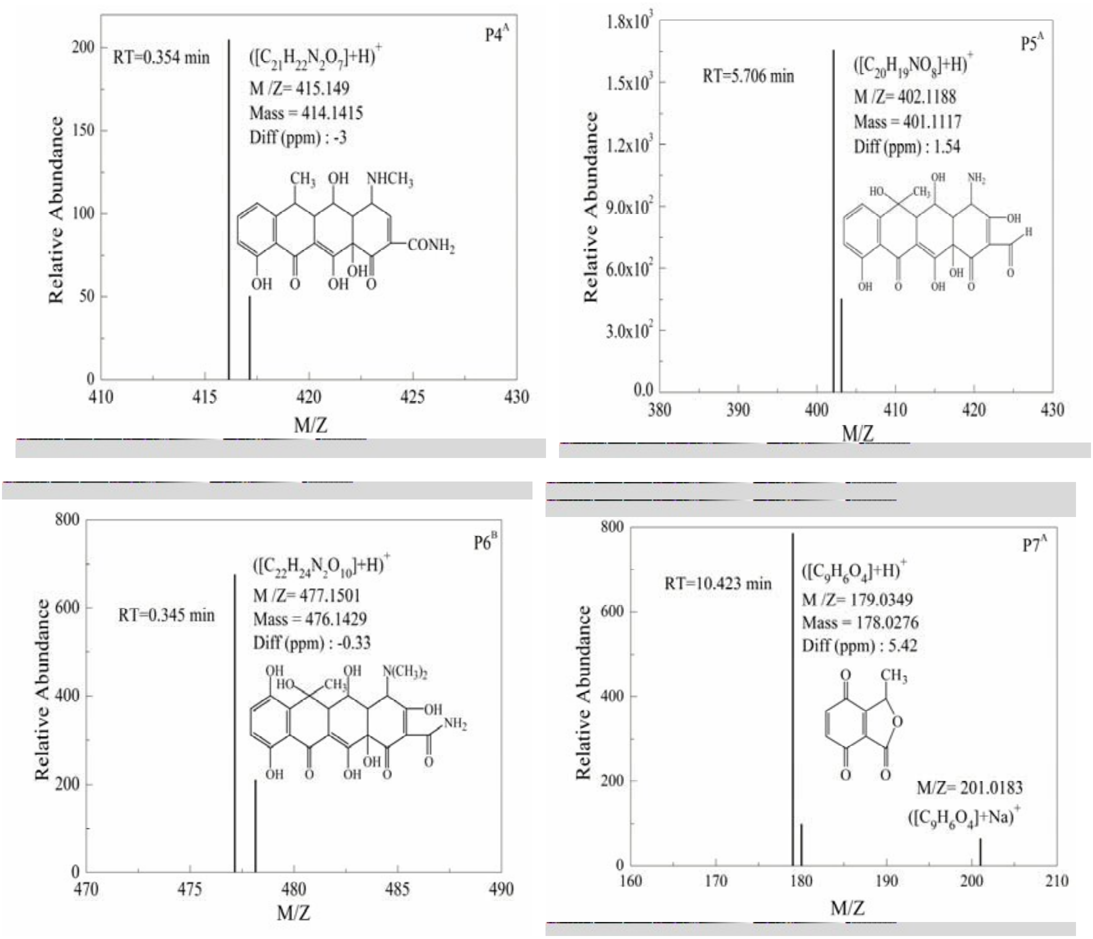

Figure 9. Product ions spectra of OTC photocatalysis sample before and after photocatalytic degradation ([45 Fe_2O_3-TiO_2 NPs] = 1 g/L, OTC: 60 mg/L, pH = 5.5, 5 h UV/vis irradiation). (superscript B: product ions detected in original OTC solution; superscript A: product ions detected in OTC solution after photocatalytic degradation).

3.6 Mechanism of Photodegradation

The mechanism of OTC degradation can be described as equations (3)-(7). Firstly, the OTC molecular was adsorbed onto the surface of Fe_2O_3-TiO_2 nanopowders. It was well known that conduction band electron (e^-) and valence band holes (h^+) are generated when aqueous TiO_2 suspension is irradiated with UV light energy.[12] However, due to the large distance between VB and CB (3.31eV), absorption of visible-light is negligible for pure TiO_2. In Fe_2O_3-TiO_2, as the band edge of Fe^{3+} is lower than TiO_2, which means that Fe^{3+} is situated in between conduction band (CB) and valence band (VB). When visible-light was illuminate on Fe_2O_3-TiO_2, the electrons excited from the valence band to forbidden band leaving holes in the valence band TiO_2. The photogenerated $e^- - h^+$ pairs can recombine in the bulk catalyst or diffuse to the catalyst particle surface and react with H_2O and O_2 molecules adsorbed there leading to the formation of reactive oxygen species (ROS) under visible light. [13] As a very strong oxidizing agent, the $\cdot OH$ radical and $\cdot O_2^-$ can oxidize most of TC antibiotics to the mineral end-products.[14-16]

$$Fe_2O_3\text{ - }TiO_2 + OTC \xrightarrow{\text{Adsorption}} (Fe_2O_3\text{-}TiO_2) - OTC \qquad (3)$$

$$Fe_2O_3\text{ - }TiO_2 + h\nu \rightarrow Fe_2O_3\text{ - }TiO_2(e^- + h^+) \qquad (4)$$

$$e^- + O_2 \rightarrow O_2^- \qquad (5)$$

$$h^+ + H_2O \rightarrow \bullet OH + H^+ \qquad (6)$$

$$OTC + h^+ / \bullet OH / O_2^- \rightarrow \text{Intermediate products} \rightarrow CO_2 \uparrow + H_2O \qquad (7)$$

At same time, Fe^{3+} species in 45 Fe_2O_3-TiO_2 NPs photocatalysts acting as h^+/e^- traps, that prevent photo-generated electron–hole recombination. h^+ and $\cdot OH$ generated in the valance band of Fe_2O_3/TiO_2 under visible light irradiation(equations 8-11) and improve photo activities for the decomposition of pollutants under visible light (equation 7). [17-19]

$$Fe^{3+} + e^- \rightarrow Fe^{2+} \qquad (8)$$

$$Fe^{2+} + O_2 \rightarrow Fe^{3+} + O_2^- \qquad (9)$$

$$Fe^{3+} + h^+ \rightarrow Fe^{4+} \qquad (10)$$

$$Fe^{4+} + OH^- \rightarrow Fe^{3+} + \bullet OH \qquad (11)$$

On the basis of LC-MS/TOF results, the degradation pathway of OTC using 45 Fe_2O_3-TiO_2 NPs is proposed in Scheme 1. In the OTC solution after photocatalytic degradation, P_2, P_3, P_4, P_5 and P_7 were founded by LC-MS/TOF. It is proposed that the photocatalytic degradation of P1 includes de-methylation and de-hydroxylation, which may produce P4.[20] Further degradation of P_2 leads to the generation of P5 via further loss of two N-methyl at aromatic ring 4 by attacking of $\cdot OH$ radicals groups, because of the low bond energy of N-C.[21] Product P6 resulted from the hydroxyl groups connected to the degraded aromatic ring 1.[22] OTC as a kind of antibiotics with stable naphthol ring as main structure and toxicity in wastewater. And some degradation byproducts of OTC have been proved to be more toxic than themselves.[21,23] The naphthol ring in P_6 have been proved easy to open in the present of ·OH radicals groups compared to other intermediate products. [24] Thus, P_7 with a partial ring-ruptured structure may stems from P_6 by further attacked by ·OH radicals, which is not reported in other literatures.

In summary, product P_5 could be formed in the reaction route of OTC ($C_{22}H_{24}N_2O_9$) → P_2 ($C_{22}H_{23}NO_9$) → P_5 ($C_{20}H_{19}NO_8$), product P_4 and P_6 could be produced as the pathways of OTC→ P_1 ($C_{21}H_{22}N_2O_9$) → P_4 ($C_{21}H_{22}N_2O_7$) and OTC → P_6 ($C_{22}H_{24}N_2O_{10}$) → P_7 ($C_9H_6O_4$). While product P_3 could be came from OTC→ P_3 ($C_{22}H_{22}N_2O_8$). It is suggested that products P_3–P_6 may be further scission to small amounts such as P_7 by ·OH radicals through naphthol ring-rupturing reactions, even these intermediate products were not detected by LC-MS/TOF. At the end of photocatalytic degradation, H_2O, CO_2 gas and other products could be obtained as final products with properly conditions (such as enough reaction time, light irradiation and photocatalyst). [25,26] However, the detail mechanism of OTC degradation will be further studied in the future.

Scheme1. Proposed degradation pathways of OTC ([45 Fe_2O_3-TiO_2 NPs] = 1 g/L, OTC: 60 mg/L, pH = 5.5, UV/vis experiment).

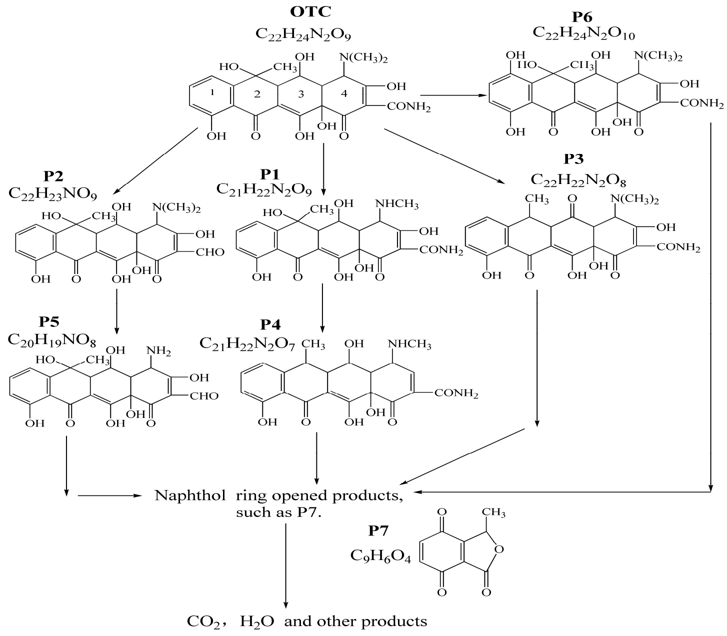

4. Conclusions

Fe_2O_3-TiO_2 NPs photocatalysts were synthesized using co-precipitation, and characterized by XRD, TEM, FT-IR and UV-vis DRS. These results shows that Fe_2O_3-TiO_2 NPs consisted of hematite Fe_2O_3 and anatase TiO_2 with particle size of 20 nm, exhibited strong absorption in visible region. Fe_2O_3-TiO_2 NPs with 45 wt% Fe_2O_3 exhibited higher photocatalytic activity than others, and all samples have more activity than pure TiO_2 under visible light. The optimized pH for remove OTC was 5.5 under both UV/Vis light due to the surface adsorption. The reusability of 45 Fe_2O_3-TiO_2 NPs has also studied, and after 3 cycles the degradation efficiency still remained at same level. The intermediate products during the photocatalytic degradation of OTC were detected by LC-MS/TOF. Five main intermediates as P_2 ($C_{22}H_{23}NO_9$), P_3 ($C_{22}H_{22}N_2O_8$), P_4 ($C_{21}H_{22}N_2O_7$) and P_7 ($C_9H_6O_4$) were formed after photocatalytic degradation, among these products, P_7 has a partial ring-ruptured structure, indicating that the complete degradation of OTC to mineral end-products. However, the more details need to be investigated in the future work to understand the mechanism.

ACKNOWLEDGMENTS

The authors would like to thank Instrumental Analysis and Research Center of Shanghai University for the experimental assistance on the TEM and XRD, Ms. Rong Jin of Institude of Nanochemistry and Nanobiology, Shanghai University for the experimental assistance on the UV-visible diffuse reflectance spectra measurement. We also greatly appreciate Ms. Qun Qian of Department of Chemistry, Shanghai University for the experimental assistance on LC-MS/TOF. This work was supported by the National Natural Science Foundation of China (Nos. 51272154), the Innovation Fund Projects of Shanghai University (Nos. sdcx2012033), the Special Research Foundation for Training and Selecting Outstanding Young Teachers of Universities in Shanghai.

REFERENCES

1 C. Zhao, H. P. Deng, Y. Li and Z. H. Liu, *J. Hazard Mater.*, 2010, 176, 884-892.

2 C. Zhao, M. Pelaez, X. Duan, H. P. Deng and K. O'Shea, *Appl Catal B-Environ.*, 2013, l 134–135, 83-92.

3 H. Liu, H. K. Shon, X. Sun, S. Vigneswaran and H. Nan, *Appl Surf Sci.*, 2011, 257, 5813-5819.

4 Y. Gao, B. H. Chen, H. L. Li and Y. X. Ma, *Mater Chem Phys.*, 2003, 80, 348–355.

5 K. P. Astam and A. B. Arghyautta, *ACS Appl. Mater. Inter.*, 2012, 4, 5022–5028.

6 X. L. Liu, P. Lv, G. X. Yao, C. C. Ma, P. W. Huo and Y. S. Yan, *Chem Eng. J.*, 2013, 217, 398–406.

7 B. M. Reddy, K. J. Ratnam and P. Saikia, *J Mol Catal A-Chem.*, 2006, 252,238–244.

8 A. K. Patra, A. Dutta and A. Bhaumik, *ACS Appl. Mater. Inter.*, 2012, 4, 5022 -5028.

9 J. G. Yu, X. J. Zhao, J. J. Yu, G. R. Zhong, J. J. Han and Q. G. Zhao, *J. Mat. Sci. Lett.*, 2001, 20, 1745-1748.

10 P. Bonamali, S. Maheshwar Sharon and N. Gyoichi, *Mater. Chem. Phys.*, 1999, 59, 254-261.

11 S. A. Sassman and L. S. Lee, *Environ Sci Technol.*, 2005, 39 (19), 7452-7459.

12 H. H. Chen, E. N. Charith and H. G. Vicki, *Chem. Rev.*, 2012, 112, 5919–5948.

13 B. Palanisamy, C. M. Babu, B. Sundaravel, S. Anandan and V. Murugesan, *J. Hazard Mater.*, 2013, 252–253, 233–242.

14 X. L. Liu, P. Lv, G. X. Yao, C. C. Ma, P. W. Huo and Y. S. Yan, *Chem Eng. J.*, 2013, 217, 398–406.

15 M. H. Khan, H. Bae and Y. J. Jin, *J. Hazard Mater.,* 2010, 181, 659–665.

16 Y. Wang, H. Zhang, J. H. Zhang, C. Liu, Q. Q. Huang, J. Wu and F. Liu, *J. Hazard Mater.*, 2011,192, 35–43.

17 M. A. Ahmed, E. E. Emad and H. G. Zarha, *J. Alloy Compd.*, 2013, 553, 19–29.

18 F. M. Dukes, E. Iuppa, B. Meyer and M. J. Shultz, *Langmuir*, 2012, 28, 16933−16940.

19 Q. L. Jin, F. Musashi and T. Hiroaki, *J. Phys. Chem. C.*, 2011, 115, 6478 –6483.

20 J. H. O. S. Pereira, V. J. P. Vilar, M. T. Borges, O. Gonz´alez, S. Esplugas and R. A. R. Boaventura, *Sol Energy*, 2011, 85, 2732-2740.

21 S. J. Jiao, S. R. Zheng, D. Q. Yin, L. H. Wang and L. Y. Chen, *J. Environ Sci*., 2008, 20, 806–813.

22 V. M. Mboula, V. Héquet, Y. Gru, R. Colin and Y. Andrès, *J. Hazard Mater*., 2012, 209–210, 355–364.

23 S. J. Jiao, S. R. Zheng, D. Q. Yin, L. H. Wang and L. Y. Chen, *Chemosphere*, 2008, 73(3), 377–382.

24 J. F. Niu, S. Y. Ding, L. W. Zhang, J. B. Zhao and C. H. Feng, *Chemosphere*, 2013, 93, 1–8.

25 X. D. Zhu, Y. J. Wang, R. J. Sun and D. M. Zhou, *Chemosphere*, 2013, 92, 925–932.

26 Z. Y. Liu, P. W. Huo, Y. Y. Luo, X. L. Liu, D. Wu, X. Gao, C. X. Li and Y. S. Yan, *J. Mol Catal A-Chem*., 2013, 378, 91-98.

Photocatalytic Degradation and Pathway of Oxytetracycline in Aqueous Solution by Fe_2O_3 - TiO_2 Nanopowders

Rong Li,[a] *Yuefa Jia ,*[a] *Jun Wu,*[a] *Qiang Zhen*[1a]

E-mail address: qzhen@staff.shu.edu.cn

Graphical abstract

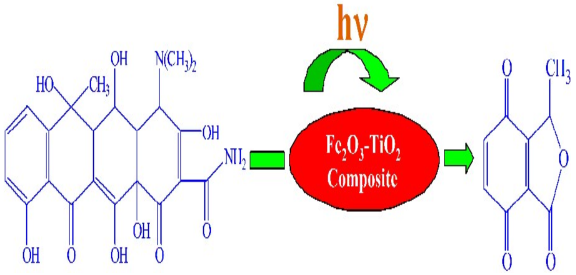

After photocatalytic degradation under UV/visible light by Fe_2O_3/TiO_2 composites, the naphthol ring of oxytetracycline ($C_{22}H_{24}N_2O_9$) destructed to partial ring-ruptured structure, such as $C_9H_6O_4$.